NJC

Accepted Manuscript

This is an *Accepted Manuscript*, which has been through the Royal Society of Chemistry peer review process and has been accepted for publication.

Accepted Manuscripts are published online shortly after acceptance, before technical editing, formatting and proof reading. Using this free service, authors can make their results available to the community, in citable form, before we publish the edited article. We will replace this *Accepted Manuscript* with the edited and formatted *Advance Article* as soon as it is available.

You can find more information about *Accepted Manuscripts* in the Information for Authors.

Please note that technical editing may introduce minor changes to the text and/or graphics, which may alter content. The journal's standard Terms & Conditions and the Ethical guidelines still apply. In no event shall the Royal Society of Chemistry be held responsible for any errors or omissions in this *Accepted Manuscript* or any consequences arising from the use of any information it contains.

ROYAL SOCIETY OF CHEMISTRY

www.rsc.org/njc

NJC

PAPER

Complexation of Hg^{2+}, CH_3Hg^+, Sn^{2+}, and $(CH_3)_2Sn^{2+}$ with phosphonic NTA derivatives

Received 00th January 20xx,
Accepted 00th January 20xx

DOI: 10.1039/x0xx00000x

www.rsc.org/

Concetta De Stefano, Claudia Foti, * Ottavia Giuffrè, and Demetrio Milea

The complex formation between Hg^{2+}, CH_3Hg^+, Sn^{2+}, and $(CH_3)_2Sn^{2+}$ and some phosphonic derivatives of nitrilotriacetic acid (NTA), namely N-(Phosphonomethyl)iminodiacetic acid (PMIDA, NTAP), N,N-Bis(phosphonomethyl)glycine (NTA2P), [Bis(phosphonomethyl)amino]methylphosphonic acid (NTA3P), has been studied by potentiometry in NaCl aqueous solution at I = 0.1 mol L^{-1} and T = 298.15 K. In order to evaluate the possible use of these ligands as sequestering agents towards the above-cited cations, some selected systems have been investigated at different ionic strengths, for a better modelling of their speciation and their binding ability in real conditions. For the same reason, the protonation enthalpy changes of the three chelants have been determined by direct calorimetric titrations, in order to define their acid-base behaviour at different temperatures. Results obtained have been compared with literature data of NTA complexes, in order to evaluate and model the effect of the number of carboxylic and/or phosphonic groups of the ligands towards their efficacy in the chelation of the investigated cations. To this aim, the stability constants of NTA with Sn^{2+} have been also determined here for the first time, since, to our knowledge, this system has never been investigated before.

Introduction

The environmental impact and the biological activity of both inorganic and organic mercury are very well known since many time, especially as concerns Hg^{2+} and CH_3Hg^+ [1-5]. The same considerations hold for organotin(IV) compounds [6, 7], while relatively few information is available for inorganic tin species (especially for Sn^{2+}) [8], though their significant presence in the environment (due to both natural occurrence and release from human activities) and the possibility of alkylation via biotic and abiotic routes make them as important as the organic forms. In this light, chemical speciation studies of inorganic and organic tin and mercury are essential to fully understand their behaviour in biologically and environmentally relevant systems, in order to minimise their negative effects. Furthermore, both tin and mercury are very important also for industry, where they can be the main products, as well as part of the process, by-products, or wastes [1, 8]. Since, in most of these cases, both tin and mercury are usually present as inorganic and/or organometal cations, their strong chelation is desirable: just three examples in the environmental, biological and industrial/technological fields may be represented by the use of chelants i) in assisted remediation processes, ii) in chelation therapy, and iii) in the recovery from wastewaters. To this aim, many efforts are addressed to the synthesis and use of new chelants, which should simultaneously be, possibly: more effective, selective, non-toxic, cheap and "eco-compatible". That is why, in the last years, the use of classical chelants like EDTA and other polyaminopolycarboxylates has been reduced, in favour of new classes of chelating agents. Among them, (poly)phosphonates are of great interest and look very promising in the replacement of old "complexones". These ligands are used in the environmental field, in biology and medicine, and for great number of technological and industrial applications (including, *e.g.*, nanomaterials), thanks to their peculiarities. For example, the simplicity of attaching the phosphonate group(s) to organic moieties encourages the synthesis of many new ligands with desired properties/structures. Moreover, phosphonates have a great chemical stability (they also resist to breakdown by enzymatic hydrolysis), but, at the same time, they generally show low toxicity, probably thanks to their structural analogies with many natural compounds [9-12]. All these aspects are (directly or not) related to their coordination chemistry, so that the comprehension of their binding ability (and, therefore, of their speciation) toward certain cations is fundamental, especially considering that, in real systems, many other competing ligands and interfering cations may be present, reducing the efficacy of the chelation process.

In the light of the above considerations, this group has recently undertaken a systematic study on the speciation of several phosphonates in aqueous solution, in different conditions [13-16]. The present contribution is aimed at investigating the effect of the replacement of the carboxylic group(s) of one of the simplest complexones (nitrilotriacetic acid, NTA) by phosphonic function(s) on the speciation and the binding ability of the ligands toward Hg^{2+}, CH_3Hg^+, Sn^{2+}, and $(CH_3)_2Sn^{2+}$. In fact, the investigated ligands, namely N-(Phosphonomethyl)-

[a] Dipartimento di Scienze Chimiche, Biologiche, Farmaceutiche ed Ambientali, Università di Messina, Viale F. Stagno d'Alcontres, 31 – 98166 Messina.

iminodiacetic acid (PMIDA, NTAP), N,N-Bis(phosphonomethyl)-glycine (NTA2P), and [Bis(phosphonomethyl)amino]-methylphosphonic acid (NTA3P), can be considered as derivatives of NTA where the three acetate groups are systematically replaced by one or more phosphonates (when together, they will be denoted in the manuscript as NTAXP, with X = 0-3, X=0 stands for NTA). Attached to the central nitrogen, NTAP has one phosphonate and two acetates, NTA2P has two phosphonates and one acetate, and NTA3P has three phosphonates (Chart 1). Measurements have been performed by potentiometry in NaCl aqueous solution at I = 0.1 mol L^{-1} and T = 298.15 K, while some selected systems have been investigated at different ionic strengths, for a better modelling of their speciation and their binding ability in real conditions. For the same reason, in order to define the acid-base behaviour of the investigated ligands at different temperatures, their protonation enthalpy changes have also been determined, by direct calorimetric titrations. Several speciation diagrams are reported in different conditions, and a series of empirical relationships are also proposed. Finally, the sequestering ability of the investigated ligands has been evaluated by the calculation of some $pL_{0.5}$ values, a semiempirical parameter recently proposed by this group for an objective quantification of the sequestering power of a given ligand toward a given cation [2].

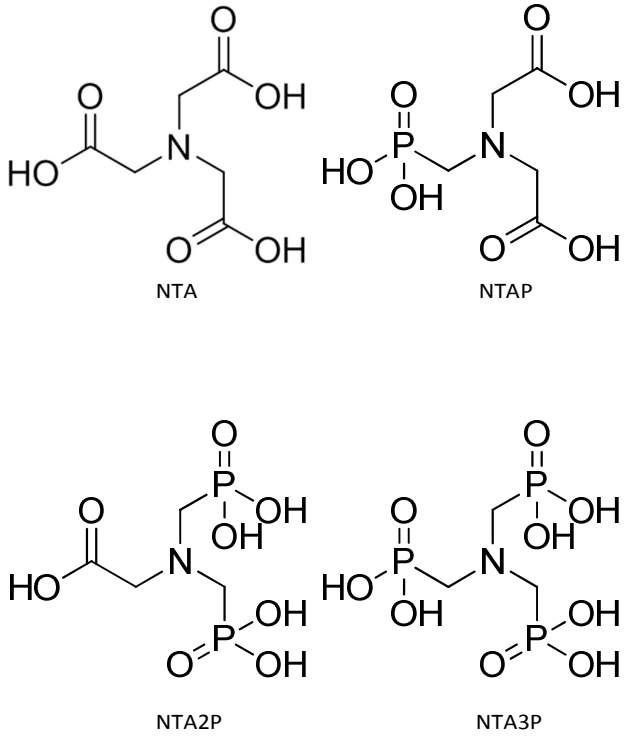

Chart 1 Structure of the investigated NTAXP ligands

Experimental

Chemicals

Nitrilotriacetic acid (NTA, H_3L), N-(Phosphonomethyl)-iminodiacetic acid (PMIDA, NTAP, H_4L), N,N-Bis(phosphonomethyl)-glycine (NTA2P, H_5L), and [Bis(phosphonomethyl)amino]-methylphosphonic acid (NTA3P, L^{6-}) were used without further purification. Solutions containing Hg^{2+}, CH_3Hg^+, Sn^{2+}, and $(CH_3)_2Sn^{2+}$ were prepared from the corresponding chlorides of the highest available purity. Particular attention was paid to the preparation of Sn^{2+} solutions, in order to avoid the oxidation of Sn(II) to Sn(IV) and the formation of sparingly soluble hydrolytic species [17], and were always used immediately after the preparation. Hg^{2+} and Sn^{2+} solutions were standardized with EDTA standard solutions, while the purity of CH_3Hg^+, $(CH_3)_2Sn^{2+}$ and that of ligands was checked potentiometrically by alkalimetric titrations, resulting always ≥ 99%. Sodium chloride aqueous solutions were prepared by weighing the pure salt previously dried in an oven at T = 383.15 K. Hydrochloric acid and sodium hydroxide solutions were prepared by diluting concentrated ampoules and were standardized against sodium carbonate and potassium hydrogen phthalate, respectively, previously dried in an oven at T = 383.15 K for 2 hours. Hydroxide solutions were preserved from atmospheric CO_2 by means of soda lime traps. All solutions were prepared with analytical grade water (ρ = 18 MΩ cm^{-1}) using grade A glassware. All products were of the highest available purity and were all purchased from Sigma Aldrich (Italy) and its various brands, except for $(CH_3)_2Sn^{2+}$, which was from Alfa Aesar.

Apparatus and procedure for potentiometric measurements

Potentiometric measurements were carried out as usual (see, *e.g.*, ref. [18]). Two different setups were used, in order to minimize systematic errors and to check the repeatability of the systems. The first setup consisted of a Model 713 Metrohm potentiometer, equipped with a half-cell glass electrode (Ross type 8101, from Thermo-Orion) and a double-junction reference electrode (type 900200, from Thermo-Orion), and a Model 765 Metrohm motorized burette. The apparatus was connected to a PC, and automatic titrations were performed using a suitable homemade computer program to control titrant delivery, data acquisition and to check for emf stability. The second setup consisted of a Metrohm model 809 Titrando apparatus controlled by Metrohm TiAMO 1.2 software equipped with combination glass electrode (Ross type 8102, from Thermo-Orion). Estimated precision was ±0.15 mV and ±0.003 mL for the emf and titrant volume readings, respectively, and was the same for both setups. Potentiometric titrations were carried out at T = 298.15 ± 0.1 K in thermostatted cells under magnetic stirring and with purified presaturated N_2 bubbling through the solution to exclude O_2 and CO_2 inside. The titrand solution consisted of different amounts of metal cation ($2.0 \le c_M$ / mmol $L^{-1} \le 5.0$, absent during measurements for the ligand

protonation), the ligand ($2.0 \le c_M$ / mmol $L^{-1} \le 7.5$), a slight excess of hydrochloric acid ($2.0 \le c_H$ / mmol $L^{-1} \le 6.0$), and NaCl in order to obtain the preestablished ionic strength values (I = 0.1 mol L^{-1}, $0.10 \le I$ / mol $L^{-1} \le 1.0$ for systems investigated at different ionic strengths). Most of the measurements were performed considering ligand-to-metal ratios in favor of the former, in order to avoid the formation of scarcely soluble species. Potentiometric measurements were carried out by titrating 25 mL of titrand solution with standard NaOH to pH ≈ 9.5-10.5. However, in the cases where the formation of sparingly soluble species was observed in some experimental conditions, the titrations were stopped at that point. For each experiment, independent titrations of strong acid solution with standard base were carried out under the same medium and ionic strength conditions as the systems to be investigated, with the aim of determining the electrode potential (E^0) and the acidic junction potential ($E_j = j_a[H^+]$). In this way, the pH scale used was the free scale, pH ≡ -log $[H^+]$, where $[H^+]$ is the free proton concentration (not activity). The reliability of the calibration in the alkaline range was checked by calculating pK_w values. For each titration, 80–100 data points were collected, and the equilibrium state during titrations was checked by adopting the usual precautions. These included checking the time required to reach equilibrium and performing back titrations.

Apparatus and procedure for calorimetric measurements

Calorimetric measurements were carried out at T = 298.150 ± 0.001 K by means of two different instruments. The first was a Tronac (model 450) isoperibolic titration calorimeter coupled with a Keithley 196 system Dmm digital multimeter; the second was a Calorimetry Science Corporation (CSC, model 4300). Both instruments were connected to a PC, and automatic titrations were performed using suitable computer programs to control calorimetric data acquisition. Measurements were performed by titrating with hydrochloric acid 50.0 mL (for Tronac) or 25 mL (for CSC) of a solution containing different amounts of ligand ($2.0 \le c_L$ / mmol $L^{-1} \le$ 7.5), sodium hydroxide (to fully deprotonate them) and the supporting electrolyte (NaCl at I = 0.1 mol L^{-1}). The titrant was delivered by 2.5 mL capacity model 1002TLL Hamilton syringes with a precision of ± 0.001 mL. For each experimental condition at least three measurements were performed. The precision of the calorimetric setups was Q ± 0.008 J for Tronac and Q ± 0.015 J for CSC, and was checked by titrating a THAM [tris(hydroxymethyl)aminomethane] solution with HCl (the heat of protonation resulted ΔH = -47.55 ± 0.04 kJ mol^{-1} in the former case, and ΔH = -47.53 ± 0.06 kJ mol^{-1} in the latter). The enthalpy of dilution was measured before each experiment under the same experimental conditions as for the calorimetric measurements. The enthalpy changes for the ionization of water used in the calculations were taken from ref. [19].

Calculations

The non-linear least squares computer program ESAB2M was used for the refinement of all the parameters of the acid–base titrations (E^0, pK_w, liquid junction potential coefficient j_a, analytical concentration of reagents). The BSTAC and STACO computer programs were used for the calculation of the protonation and complex formation constants. Both programs can deal with measurements at different ionic strengths. Some calculations have also been performed by the Hyperquad 2013 program, in order to check and confirm results obtained by previous programs. The LIANA computer program was used to fit the potentiometric data through the equations reported below. The ES4ECI program was used to draw the speciation and sequestration diagrams and to calculate the species formation percentages. The calorimetric data were analysed by the ES5CMI and the HypDH computer programs. Further details on the computer programs used are given in ref. [20] (those relative to Hyperquad and HypDH may be found in ref. [21]).

Hydrolysis (q = 0, r < 0) constants of cations (M^{m+}), protonation (p = 0) constants of the ligands (L^{l-}) and complex formation constants are given according to the following overall equilibrium:

$$p\,M^{m+} + q\,L^{l-} + r\,H^{+} = M_pL_qH_r^{(mp-lq+r)} \qquad \log \beta_{pqr} \qquad (1)$$

If not necessary, charges along the manuscript are omitted for simplicity. All complex formation constants, concentrations and ionic strengths are expressed in the molar (c, mol L^{-1}) concentration scale.

Measurements at different ionic strengths have been modelled by an Extended Debye – Hückel (EDH) type equation:

$$\log \beta_{pqr} = \log {}^{T}\beta_{pqr} - z^* \, 0.51 \, I^{1/2} \, (1 + 1.5 \, I^{1/2})^{-1} + C\,I \qquad (2)$$

where

$$z^* = \Sigma(\text{charges})^2_{\text{reactants}} - \Sigma(\text{charges})^2_{\text{products}} \qquad (3)$$

and C is an empirical parameter. If not differently specified, uncertainties are given ± 95% confidence interval (c.i.).

Results and discussion

Acid-base properties of cations and ligands

The study of the speciation and the complex formation of various metal/ligand systems requires a preliminary knowledge of the acid – base properties of both the metal cations (hydrolysis) and the ligands (protonation) in the same experimental conditions of the system to be investigated. Concerning the hydrolysis of cations and the protonation of NTA, these data were taken from previous studies: ref. [22] for Hg^{2+}, ref. [23] for CH_3Hg^+, ref. [17] for Sn^{2+}, ref. [24] for $(CH_3)_2Sn^{2+}$, and ref. [25] for NTA. Since most of the investigated cations form quite stable species with chloride too, the corresponding formation equilibria have been explicitly taken into account during calculations (taken from the same refs.).

Concerning the phosphonic ligands investigated, NTAP, NTA2P, and NTA3P, their protonation constants have been experimentally determined in this work at different ionic

Table 1. Experimental protonation constants of NTAP, NTA2P e NTA3P in NaCl at different ionic strengths and T = 298.15 K

Ligand	I / mol L^{-1}	log β_{011} [a]	log β_{012} [a]	log β_{013} [a]	log β_{014} [a]
NTAP	0.102	10.52 ± 0.01	16.07 ± 0.02	18.05 ± 0.04	20.05 ± 0.04
	0.244	10.23 ± 0.01	15.67 ± 0.02	17.86 ± 0.02	19.43 ± 0.04
	0.469	10.09 ± 0.01	15.44 ± 0.01	17.51 ± 0.02	19.33 ± 0.02
	0.940	9.81 ± 0.02	15.03 ± 0.02	17.34 ± 0.04	19.11 ± 0.04
NTA2P	0.114	11.28 ± 0.02	17.64 ± 0.02	22.60 ± 0.02	24.68 ± 0.04
	0.250	11.08 ± 0.01	17.24 ± 0.01	22.03 ± 0.02	23.93 ± 0.02
	0.480	10.88 ± 0.02	16.89 ± 0.02	21.60 ± 0.04	23.48 ± 0.06
	0.916	10.67 ± 0.01	16.50 ± 0.02	21.08 ± 0.02	22.90 ± 0.02
NTA3P	0.101	11.90 ± 0.07	18.80 ± 0.07	24.48 ± 0.08	28.87 ± 0.08

[a] log β_{01r} refer to equilibria: L + r H = LH_r, charges omitted for simplicity, ± 95% confidence interval.

strengths (0.10 ≤ I / mol L^{-1} ≤ 1.0, only I = 0.1 mol L^{-1} in the case of NTA3P) and are reported in Table 1. As observed, in the experimental conditions investigated, only four protonation constants have been determined for all ligands, independently of the fact that NTA2P and NTA3P could formally have one and two additional protonation steps, respectively. This is consistent with literature findings [9, 26, 27], and it is due to the fact that their fifth (and sixth for NTA3P) protonation step occurs significantly only at pH < 3.0. Nevertheless, for NTA3P, log β_{015} = 31.5 ± 0.3 can be given as a tentative value at I = 0.1 mol L^{-1}. The protonation constants determined for NTAP and NTA2P at different ionic strengths have been modelled by eq. (2). Its refined parameters, including the protonation constants at infinite dilution, are reported in Table 2, while values calculated ad different ionic strengths are in Table 3.

Table 2. Refined parameters of eq. (2) for the modelling of the dependence of the protonation constants of NTAP and NTA2P on ionic strength, in $NaCl_{(aq)}$ and at T = 298.15 K

L	r	log $^{T}\beta_{01r}$ [a, b]	z*	C [b]
NTAP	1	11.40 ± 0.05	8	0.04 ± 0.01
	2	17.63 ± 0.06	14	0.27 ± 0.01
	3	20.10 ± 0.09	18	0.96 ± 0.01
	4	22.14 ± 0.04	20	1.09 ± 0.02
NTA2P	1	12.44 ± 0.06	10	0.27 ± 0.01
	2	19.71 ± 0.05	18	0.46 ± 0.01
	3	25.35 ± 0.06	24	0.63 ± 0.02
	4	27.82 ± 0.06	28	0.79 ± 0.01

[a] log β_{01r} refer to equilibria: L + r H = LH_r, charges omitted for simplicity; [b] ± 95% confidence interval.

As already mentioned in the introduction, the protonation enthalpy changes of the investigated phosphonic ligands have been determined by direct calorimetric titrations, in $NaCl_{(aq)}$ at I = 0.1 mol L^{-1}, at T = 298.15 K (Table 4). The first protonation step is exothermic for all ligands, while the successive are slightly endothermic (values in Table refer to overall equilibria). As happened for the protonation constants, for NTA3P, a rough protonation enthalpy change value can be given for the fifth step: ΔH_{015} = -16.2 ± 0.9. By means of the van't Hoff equation, enthalpy changes reported in Table 4 may be exploited to calculate the protonation constants of the investigated ligands at other temperatures than T = 298.15 K, allowing the evaluation of the effect of temperature on their acid-base behaviour and, therefore, on their speciation. Both the ionic strength and temperature effects can be better appreciated looking at Figures 1 and 2 where, for example, the distribution diagrams of NTA2P (de)protonated species are reported at T = 298.15 K and different I values (*i.e.*, I = 0.1 and 1.0 mol L^{-1}, Figure 1), and those of NTA3P at I = 0.1 mol l^{-1} and different temperatures (*i.e.*, T = 298.15 and 310.15 K, Figure 2).

Table 4. Overall protonation enthalpy changes of NTAP, NTA2P, and NTA3P, in $NaCl_{(aq)}$ at I = 0.1 mol L^{-1} and at T = 298.15 K

Ligand	ΔH_{011} [a]	ΔH_{012} [a]	ΔH_{013} [a]	ΔH_{014} [a]
NTAP	-11.7 ± 0.3	-8.7 ± 0.3	-5.5 ± 0.7	—
NTA2P	-16.0 ± 0.4	-12.2 ± 0.5	-7.8 ± 0.5	-6.9 ± 0.7
NTA3P	-35.8 ± 0.9	-26.9 ± 0.1	-22.1 ± 0.1	-17.5 ± 0.2

[a] ΔH_{01r} refer to equilibria: L + r H = LH_r, charges omitted for simplicity, ± 95% confidence interval.

Table 3. Protonation constants of NTAP and NTA2P calculated by eq. (2) in NaCl at different ionic strengths and T = 298.15 K

Ligand	I / mol L^{-1}	log β_{011} [a]	log β_{012} [a]	log β_{013} [a]	log β_{014} [a]
NTAP	0.10	10.52 ± 0.04	16.12 ± 0.04	18.23 ± 0.08	20.06 ± 0.04
	0.25	10.24 ± 0.04	15.66 ± 0.04	17.72 ± 0.06	19.50 ± 0.03
	0.50	10.01 ± 0.03	15.31 ± 0.04	17.43 ± 0.05	19.18 ± 0.04
	1.00	9.80 ± 0.07	15.04 ± 0.08	17.39 ± 0.09	19.15 ± 0.08
NTA2P	0.10	11.37 ± 0.05	17.79 ± 0.06	22.79 ± 0.05	24.84 ± 0.05
	0.25	11.05 ± 0.04	17.20 ± 0.04	22.01 ± 0.04	23.94 ± 0.04
	0.50	10.83 ± 0.03	16.79 ± 0.04	21.46 ± 0.04	23.32 ± 0.04
	1.00	10.67 ± 0.07	16.50 ± 0.07	21.09 ± 0.08	22.90 ± 0.08

[a] log β_{01r} refer to equilibria: L + r H = LH_r, charges omitted for simplicity, ± 95% confidence interval.

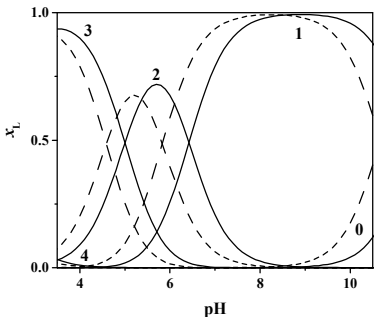

Figure 1. Distribution diagram of $(NTA2P)H_r$ species, at T = 298.15 K, in $NaCl_{(aq)}$ at I = 0.1 (solid lines) and 1.0 (dashed lines) mol L^{-1}. c_L = 0.005 mol L^{-1}. Indexes in figure refer to the $(NTA2P)H_r$ species: *e.g.*, 2 stands for $(NTA2P)H_2$.

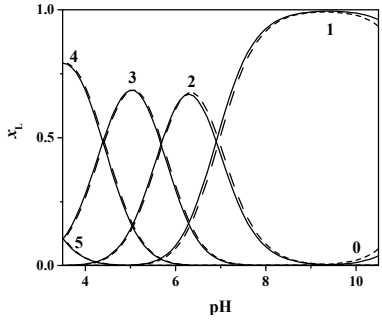

Figure 2. Distribution diagram of $(NTA3P)H_r$ species, at I = 0.1 mol L^{-1} in $NaCl_{(aq)}$, at T = 298.15 (solid lines) and 310.15 K (dashed lines). c_L = 0.005 mol L^{-1}. Indexes in figure refer to the $(NTA3P)H_r$ species: *e.g.*, 2 stands for $(NTA3P)H_2$.

As observed, increasing ionic strength determines in NTA2P a shift of curves of various species toward more acidic pHs (about 0.5-1.0 units), while small temperature changes (about 10-15 degrees) do not significantly alter the speciation profiles of the protonated species of NTA3P.

Hg^{2+} complexes

The analysis of experimental data of various Hg^{2+} / NTAXP systems gave results reported in Table 5. All the three investigated ligands form the same four species, namely MLH_2, MLH, ML, and MLOH. Their stability is quite similar for the three ligands, showing a slight increase with the increasing of the number of phosphonic moieties. This is much more evident comparing the stability of the Hg(NTAXP) species (X = 1-3) with that of the analogue HgNTA, which is, in the same conditions (*i.e.*, I = 0.1 mol L^{-1} and T = 298.15 K), log β_{110} = 14.3 [26]. The importance of these complexes in terms of speciation can be better appreciated in Figures 3a-c, where the distribution diagrams of Hg^{2+} species are reported in systems containing NTAP (3a), NTA2P (3b) and NTA3P (3c), respectively. In those conditions, Hg^{2+} is almost entirely complexed by these ligands at pH > 6.0, while, below this value, Hg^{2+} is present in significant amounts as uncomplexed by the three NTAXP (dashed lines), mainly as chloride species. Due to the fact that chloride concentration is 50 times that of NTAXP ligands (c_{Cl} = 0.1 moL^{-1}, c_L = 0.002 moL^{-1}), this is not surprising, but, on the contrary, worth mentioning is that, $Hg_p(NTAXP)_qH_r$ species are still formed.

Table 5. Stability constants of $Hg(NTAXP)H_r$ species, in $NaCl_{(aq)}$ at I = 0.1 mol L^{-1} and at T = 298.15 K

Ligand	log β_{112} [a]	log β_{111} [a]	log β_{110} [a]	log $\beta_{11\text{-}1}$ [a]
NTAP	29.64 ± 0.09	25.19 ± 0.04	19.96 ± 0.02	9.84 ± 0.02
NTA2P	31.87 ± 0.06	26.98 ± 0.01	21.22 ± 0.02	11.05 ± 0.03
NTA3P	32.94 ± 0.08	27.65 ± 0.02	21.27 ± 0.03	11.19 ± 0.05

[a] log β_{11r} refer to equilibria: M + L + r H = MLH_r, charges omitted for simplicity, ± 95% confidence interval.

CH_3Hg^+ complexes

Also in the case of CH_3Hg^+, the three investigated ligands showed similar speciation schemes. The kind of species determined, together with their corresponding stability constants, are reported in Table 6. In the same Table, the stability constants of the analogue NTA complexes, taken from literature [28], are also reported to facilitate comparisons

Table 6. Stability constants of $(CH_3Hg)(NTAXP)H_r$ species, in $NaCl_{(aq)}$ at I = 0.1 mol L^{-1} and at T = 298.15 K

Ligand	log β_{112} [a]	log β_{111} [a]	log β_{110} [a]	log $\beta_{11\text{-}1}$ [a]
NTA [b]	--	15.98	9.03	-1.57
NTAP	--	16.86 ± 0.05	9.97 ± 0.01	-0.67 ± 0.01
NTA2P	24.22 ± 0.07	18.00 ± 0.07	10.48 ± 0.04	--
NTA3P	25.28 ± 0.07	18.65 ± 0.05	10.97 ± 0.04	--

[a] log β_{11r} refer to equilibria: M + L + r H = MLH_r, charges omitted for simplicity, ± 95% confidence interval; [b] from ref. [28].

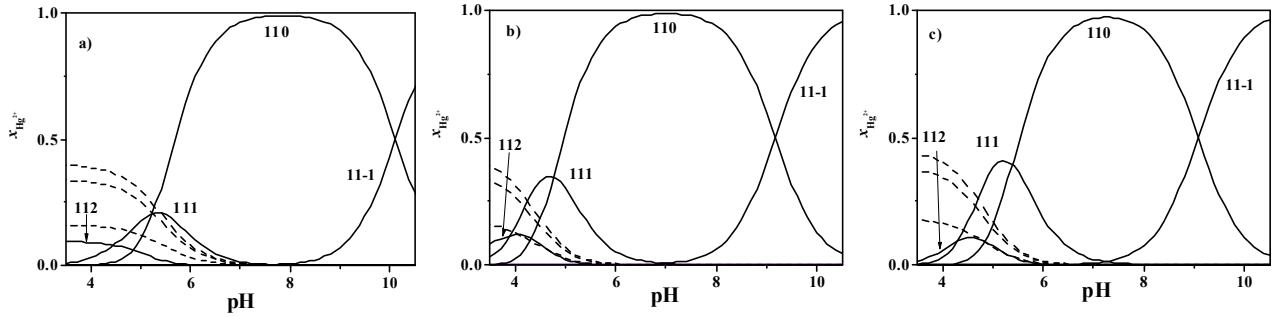

Figure 3. Distribution of $Hg_p(NTAXP)_qH_r$ species in the Hg^{2+} / NTAP (a), Hg^{2+} / NTA2P (b), and Hg^{2+} / NTA3P (c) systems, in $NaCl_{(aq)}$ at I = 0.1 mol L^{-1} and T = 298.15 K. c_M = 0.001 mol L^{-1}, c_L = 0.002 mol L^{-1}. Indexes in figures refer to the $Hg_p(NTAXP)_qH_r$ species: *e.g.*, 111 stands for Hg(NTAXP)H. Dashed lines refer to Hg^{2+} uncomplexed by NTAXP ligands.

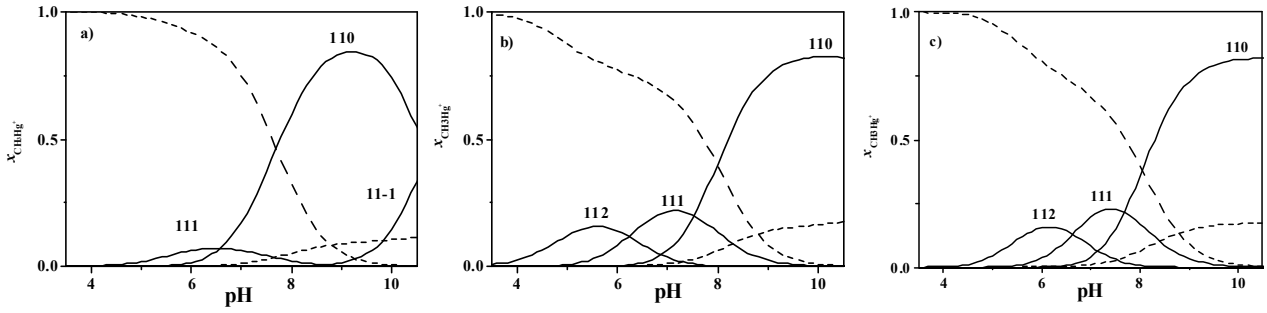

Figure 4. Distribution of $(CH_3Hg)_p(NTAXP)_qH_r$ species in the CH_3Hg^+ / NTAP (a), CH_3Hg^+ / NTA2P (b), and CH_3Hg^+ / NTA3P (c) systems, in $NaCl_{(aq)}$ at I = 0.1 mol L^{-1} and T = 298.15 K. c_M = 0.001 mol L^{-1}, c_L = 0.002 mol L^{-1}. Indexes in figures refer to the $(CH_3Hg)_p(NTAXP)_qH_r$ species: *e.g.*, 111 stands for $CH_3Hg(NTAXP)H$. Dashed lines refer to CH_3Hg^+ uncomplexed by NTAXP ligands.

(a further dinuclear M_2L species with log β_{210} = 15.09 is also reported for NTA by authors in the same conditions). As can be noted, the ML and MLH species are common for all the ligands. Besides, depending on the charge of the fully deprotonated anions, NTA and NTAP (respectively L^{3-} and L^{4-}) also form the MLOH species, while NTA2P and NTA3P (formally L^{5-} and L^{6-}) form the diprotonated MLH_2. Also in this case, their importance for CH_3Hg^+ speciation in systems containing these ligands can be better appreciated in Figure 4, where the corresponding distribution diagrams are reported. In the conditions used for both Figures 3 and 4, at pH > 6.0 Hg^{2+} is almost entirely complexed by the three ligands, while, in the whole pH range considered, the fraction of CH_3Hg^+ complexed by NTAXP ligands never reach x = 1 (*i.e.*, free CH_3Hg^+ is always present, as chloride or hydrolytic species).

Sn^{2+} complexes

Despite the importance and the vast use of Sn^{2+} in several fields, relatively few thermodynamic data are available in literature on its speciation and on the stability of its complexes with various ligands [26, 29-33]. This is mainly due to a series of experimental difficulties in working with this cation (*e.g.*, strong hydrolysis, oxidation to Sn^{4+}, formation of precipitates). For example, we have not been able to find any literature data on the stability of its complexes neither with the NTAXP ligands investigated in the present work, nor with the most common NTA. That is why, in addition to NTAXP ligands, we also decided to investigate the speciation of Sn^{2+} in the presence of NTA, in order to have a clearer picture of the binding ability of these complexons toward this cation. Results obtained are shown in Table 7. As can be immediately noted, in the experimental conditions investigated, no simple $Sn(NTA)H_r$ species are observed, in favour of the dimeric $Sn(NTA)_2H_2$, $Sn(NTA)_2H$, and $Sn(NTA)_2$. The tendency to form dimeric species instead of simple MLH_r is not unusual neither for NTA, nor for Sn^{2+}, especially when ligand to metal ratios higher than unit (*i.e.*, c_L:c_M > 1, like in this case) are used during the experiments, usually to avoid the formation of sparingly soluble species (which for Sn^{2+} are very frequent). The speciation diagram of Sn^{2+} in the presence of NTA is shown in Figure 5. The part of the diagram at pH > 8.0 is shadowed, as warning: above this pH, the formation of sparingly soluble species, generally $Sn(OH)_{2(s)}$, may occur in the Sn^{2+} / NTA system, depending on the experimental conditions (*e.g.*, total metal and ligand concentrations, metal to ligand ranges, etc.). So, particular attention must be paid when considering Sn^{2+} speciation at high pHs, independently of the ligands present. In fact, though NTA is able to maintain Sn^{2+} in solution over a wider pH range than usual (generally in the absence of strong ligands Sn^{2+} precipitation already occurs at pH < ~4.0, depending on its concentration, for $Sn(OH)_{2(s)}$ at T = 298.15 K and infinite dilution it is log K_{s0} = 26.3), small changes in the conditions may determine the formation of precipitate or not.

Table 7. Stability constants of $Sn_p(NTAXP)_qH_r$ species, in $NaCl_{(aq)}$ at I = 0.1 mol L^{-1} and at T = 298.15 K

Species			log β_{pqr} [a]	
p q r	NTA	NTAP	NTA2P	NTA3P
1 1 2	--	--	34.10 ± 0.02	28.45 ± 0.08
1 1 1	--	20.78 ± 0.04	29.20 ± 0.02	24.18 ± 0.06
1 1 0	--	16.89 ± 0.03	18.96 ± 0.04	18.23 ± 0.02
1 1 -2	--	-2.75 ± 0.05	--	--
1 2 2	29.25 ± 0.03	--	--	--
1 2 1	26.87 ± 0.02	--	--	--
1 2 0	17.95 ± 0.05	--	--	--

[a] log β_{pqr} refer to equilibria: p M + q L + r H = $M_pL_qH_r$, charges omitted for simplicity, ± 95% confidence interval.

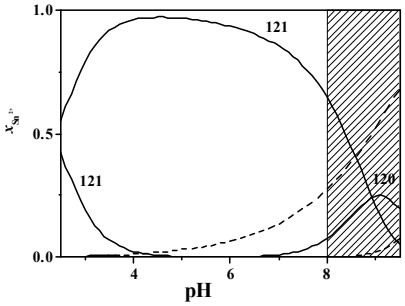

Figure 5. Distribution of $Sn_p(NTA)_qH_r$ species in the Sn^{2+} / NTA system, in $NaCl_{(aq)}$ at I = 0.1 mol L^{-1} and T = 298.15 K. c_M = 0.001 mol L^{-1}, c_L = 0.002 mol L^{-1}. Indexes in figures refer to the $Sn_p(NTA)_qH_r$ species: *e.g.*, 121 stands for Sn(NTA)H. Dashed lines refer to Sn^{2+} uncomplexed by NTA. Shadowed range refer to the possible formation of sparingly soluble species.

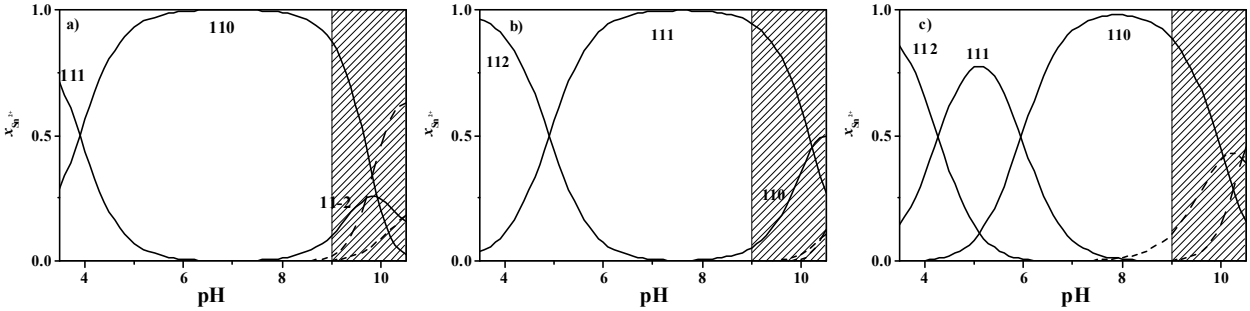

Figure 6. Distribution of $Sn_p(NTAXP)_qH_r$ species in the Sn^{2+} / NTAP (a), Sn^{2+} / NTA2P (b), and Sn^{2+} / NTA3P (c) systems, in $NaCl_{(aq)}$ at I = 0.1 mol L^{-1} and T = 298.15 K. c_M = 0.001 mol L^{-1}, c_L = 0.002 mol L^{-1}. Indexes in figures refer to the $Sn_p(NTAXP)_qH_r$ species: *e.g.*, 111 stands for Sn(NTAXP)H. Dashed lines refer to Sn^{2+} uncomplexed by NTAXP ligands.

Paying attention to the species formed by the investigated phosphonates, it is possible to note in Table 7 that, like Hg^{2+} and CH_3Hg^+, also Sn^{2+} forms the simple ML and MLH with all the three NTAXP ligands, as well as the MLH_2 species with NTA2P and NTA3P. Only in the case of NTAP, a different speciation is observed for Sn^{2+} with respect to Hg^{2+} and CH_3Hg^+, since the di-hydroxo species $ML(OH)_2$ is obtained for the former cation in spite of the simple hydrolytic MLOH formed by the last two. This is not surprising if one takes into account the very strong hydrolysis of Sn^{2+} (first hydrolytic species are already formed at pH ~2.5-3.0), which facilitate the formation of less protonated species. Probably, considering the pH range where this species is formed and the acid-base behaviours of both NTAP and Sn^{2+}, one may assume that the effective formation equilibrium of the $ML(OH)_2$ species occurs between the fully deprotonated ligand and the $Sn(OH)_2$. Of course, apart from structural considerations, considering one formation equilibrium or another does not alter the speciation profile of the system. The speciation diagrams of Sn^{2+} in systems containing the three NTAXP ligands are shown in Figure 6 (the same considerations done for the shadowed pH range in Figure 5 hold also in this case for pH > 9.0). As in the case of Hg^{2+}, Sn^{2+} is almost entirely complexed by all NTAXP ligands up to pH ~8.0. Nevertheless, while NTAP and NTA2P show the formation of a predominating species (ML and MLH, respectively) in the mid-acidic – mid-basic pH range, the formation curves of each NTA3P species are narrow and reflect, in some way, those of the protonated species of the ligand. This could be ascribed to the fact that complexation of Sn^{2+} by the less protonated phosphonates (*i.e.*, NTAP, NTA2P) causes a strong protons' displacement already at relatively low pHs, while this displacement is less marked in the more protonated NTA3P.

$(CH_3)_2Sn^{2+}$ complexes

The last systems investigated are those with $(CH_3)_2Sn^{2+}$, chosen as representative of the environmentally, industrially and biologically relevant class of organotin(IV) cations. Moreover, its complexes with NTA have already been studied in detail by this group in similar conditions [34], so that comparisons between NTA and the NTAXP ligands investigated here can be easier. The analysis of experimental data gave the results reported in Table 8 (where literature data on NTA are tabled too). As observed, all the three phosphonates form the same kind of species, namely MLH, ML, and MLOH. In addition, NTA2P and NTA3P also form the di-protonated MLH_2, while the di-hydrolytic $ML(OH)_2$ is only observed in the case of NTAP and NTA3P. This last species is not formed by NTA2P in the investigated conditions, where the most deprotonated species determined is the MLOH. To better comprehend how $(CH_3)_2Sn^{2+}$ speciation is affected by the formation of NTAXP complexes, its distribution diagrams in the presence of the three ligands are reported in Figure 7. Interestingly, differences in the binding ability of the three NTAXP are more marked for $(CH_3)_2Sn^{2+}$ than for other cations (as usual, conditions of diagrams in Figure 7 are the same of those in Figures 3-6). In the presence of NTAP, the $(CH_3)_2Sn(OH)_2$ species is preponderant in the alkaline pH range, hampering the formation of significant amounts of the MLOH and, to less extent, the $ML(OH)_2$ species (which, however, are formed in higher percentages in other conditions). In the case of NTA2P, the formation of the ML species dominates $(CH_3)_2Sn^{2+}$ speciation in the pH range ~5.0 – 10.0. As a consequence, the formation of MLOH starts at pH ~9.0-9.5 (together with simple hydrolytic species), resulting in the lack of any $ML(OH)_2$ at pH < 10.5 (end of diagram). Finally, NTA3P strongly inhibits the formation of simple hydrolytic species, complexing all $(CH_3)_2Sn^{2+}$ in the whole pH range, with high formation percentages of all species (relatively less important in the diagram is the MLOH, but it reaches 30-40%).

Table 8. Stability constants of $((CH_3)_2Sn)(NTAXP)_qH_r$ species, in $NaCl_{(aq)}$ at I = 0.1 mol L^{-1} and at T = 298.15 K

Species			log β_{pqr} [a]	
p q r	NTA [b]	NTAP	NTA2P	NTA3P
1 1 2	--	--	23.89 ± 0.02	28.52 ± 0.03
1 1 1	12.36	16.99 ± 0.01	20.90 ± 0.01	25.22 ± 0.04
1 1 0	10.17	13.65 ± 0.01	16.42 ± 0.01	19.46 ± 0.07
1 1 -1	3.15	3.26 ± 0.06	5.66 ± 0.05	11.53 ± 0.08
1 1 -2	--	-5.61 ± 0.01	--	3.46 ± 0.09

[a] log β_{11r} refer to equilibria: M + L + r H = MLH_r, charges omitted for simplicity, ± 95% confidence interval; [b] from ref. [34].

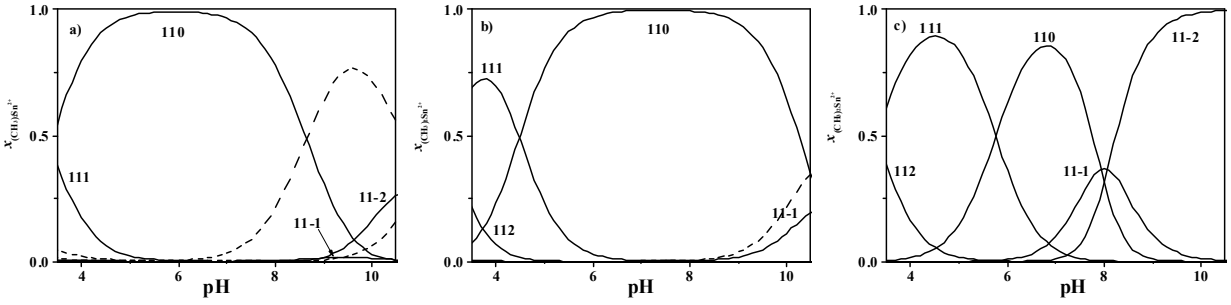

Figure 7. Distribution of $((CH_3)_2Sn)_p(NTAXP)_qH_r$ species in the $(CH_3)_2Sn^{2+}$ / NTAP (a), $(CH_3)_2Sn^{2+}$ / NTA2P (b), and $(CH_3)_2Sn^{2+}$ / NTA3P (c) systems, in $NaCl_{(aq)}$ at I = 0.1 mol L^{-1} and T = 298.15 K. c_M = 0.001 mol L^{-1}, c_L = 0.002 mol L^{-1}. Indexes in figures refer to the $((CH_3)_2Sn)_p(NTAXP)_qH_r$ species: *e.g.*, 111 stands for $((CH_3)_2Sn)(NTAXP)H$. Dashed lines refer to $(CH_3)_2Sn^{2+}$ uncomplexed by NTAXP ligands.

Ionic strength effect on complexation

As specified above, some systems have also been investigated at different ionic strength values. In particular, for the NTAP systems with Hg^{2+}, CH_3Hg^+, and $(CH_3)_2Sn^{2+}$, measurements at different ionic strengths ($0.10 \le I$ / mol $L^{-1} \le 1.0$) have been performed. The simultaneous analysis of experimental data at different I values by the BSTAC and STACO programs allowed the determination of the stability constants of the $Hg_p(NTAP)_qH_r$, $(CH_3Hg)_p(NTAP)_qH_r$, and $((CH_3)_2Sn)_p(NTAP)_qH_r$ species at infinite dilution, as well as the corresponding C parameters of eq. (2) for their dependence on ionic strength, as reported in Table 9. For a more immediate visualization of the ionic strength effect on the speciation of these systems, the distribution diagrams of Hg^{2+}, CH_3Hg^+, and $(CH_3)_2Sn^{2+}$ species at I = 1.0 mol L^{-1} are reported in Figure 8 in the same metal and ligand concentrations of analogous systems plotted at I = 0.1 mol L^{-1} in Figures 3a, 4a, and 7a, respectively. It can be immediately noted that the speciation of the three cations at I = 0.1 mol L^{-1} and I = 1.0 mol L^{-1} is significantly different. In the case of Hg^{2+} (Figures 3a and 8a), the protonated MLH_2 and MLH species show greater formation percentages in the latter case than in the former, limiting the formation of the ML to a narrower pH range and shifting both the ML and MLOH formation toward more basic pHs. Concerning CH_3Hg^+ (Figures 4a and 8b), which form stable chloride complexes, the greater concentration of this anion at I = 1.0 mol L^{-1} as a huge influence on speciation: no significant amounts of $(CH_3Hg)_p(NTAP)_pH_q$ are observed at pH < ~7.0, where chloride complexes are dominant. Only in the alkaline range, where the NTAP deprotonation favour complexation, the ML and MLOH species are formed in high percentages (> 50%). Finally, in the case of $(CH_3)_2Sn^{2+}$ (Figures 7a and 8c), increasing ionic strength determines a greater formation percentage of the MLOH and $ML(OH)_2$ species, lowering the amount of simple hydroxo-species of dimethyltin(IV) cation (< 50%).

Table 9. Refined parameters of eq. (2) for the modelling of the dependence of the stability constants of various $M_p(NTAP)_qH_r$ species on ionic strength ($0 < I$ / mol $L^{-1} \le 1.0$), in $NaCl_{(aq)}$ and at T = 298.15 K

Species	$\log {}^T\beta_{pqr}$ [a, b]	z^*	C [b]
p q r		Hg^{2+}	
1 1 2	32.4 ± 0.4	22	5.7 ± 0.6
1 1 1	27.3 ± 0.3	20	5.3 ± 0.4
1 1 0	21.8 ± 0.2	16	2.5 ± 0.4
1 1 -1	10.9 ± 0.1	10	1.2 ± 0.2
		CH_3Hg^+	
1 1 1	18.4 ± 0.2	14	0.30 ± 0.11
1 1 0	10.8 ± 0.1	8	0.11 ± 0.08
1 1 -1	-0.7 ± 0.2	0	0
		$(CH_3)_2Sn^{2+}$	
1 1 1	19.0 ± 0.1	20	1.3 ± 0.2
1 1 0	15.4 ± 0.1	16	0.64 ± 0.09
1 1 -1	4.2 ± 0.1	10	1.8 ± 0.1
1 1 -2	-5.5 ± 0.1	2	0.20 ± 0.11

[a] log β_{pqr} refer to equilibria: p M + q NTAP + r H = $M_p(NTAP)_qH_r$, charges omitted for simplicity; [b] ± 95% confidence interval.

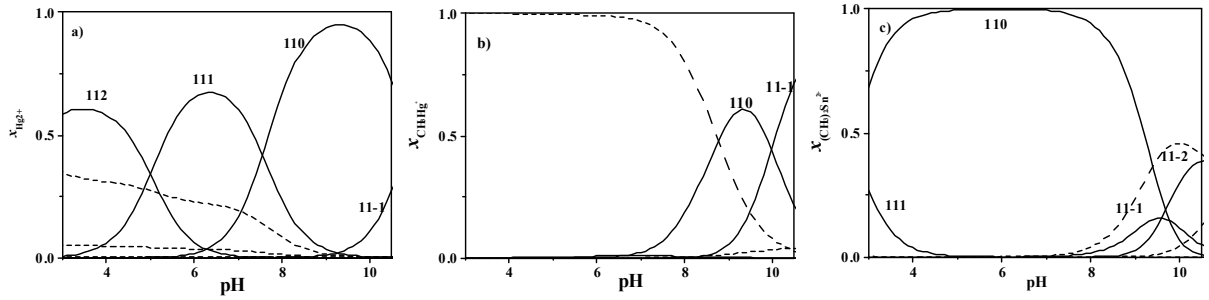

Figure 8. Distribution of $M_p(NTAP)_qH_r$ species in the Hg^{2+} / NTAP (a), CH_3Hg^+ / NTAP (b), and $(CH_3)_2Sn^{2+}$ / NTAP (c) systems, in $NaCl_{(aq)}$ at I = 1.0 mol L^{-1} and T = 298.15 K. c_M = 0.001 mol L^{-1}, c_L = 0.002 mol L^{-1}. Indexes in figures refer to the $M_p(NTAP)_qH_r$ species: *e.g.*, 111 stands for M(NTAP)H. Dashed lines refer to the cation uncomplexed by NTAP.

Sequestering ability

As known, one of the main reasons of the vast number of fields of application of complexones is their ability to sequester metal (and other) cations. From this point of view, the efficacy of a chelant depends not only on its binding ability toward a given cation *tout-court*, but it is function of the speciation of both the chelant and the metal in a given condition. In fact, many real systems are multicomponent, and many other interfering ligands and cations are usually present, leading to a great number of competing reactions with both the metal and chelants of interest and affecting deeply the efficacy of the whole sequestration process [35-40]. As a consequence, the simple comparison of the stability constants of the metal complexes formed by a metal cation with two or more ligands is not sufficient to evaluate if one ligand is more effective as chelant than another. Analogously, this simple comparison is not sufficient neither in the case where it is necessary to assess if the chelation by a given ligand is stronger toward one or another cation. Furthermore, many metal/ligand systems rarely form only one species, and even in this case, it could not necessarily show the same stoichiometry of that formed in the systems to compare. Starting from these points, many efforts have been done during the years to give efficacious instruments to people (expert or not) interested in the quantification of the sequestering ability of ligands toward metal cations. To this aim, this group proposed and uses the calculation of a semiempirical parameter, the $pL_{0.5}$ (formerly pL_{50}), which represent the total concentration (as antilogarithm) of ligand necessary to sequester 50% (in mole fraction, $x = 0.5$) of a given cation when it is present in trace in a given system, whatever its composition and complexity is. Its calculation is based on a sort of dose-response, sigmoidal Boltzmann-type equation where the fraction of a cation complexed by a specific ligand is expressed as a function of the concentration of the latter (as $pL \equiv -\log c_L$):

$$x = \frac{1}{1 + 10^{\,pL - pL_{0.5}}} \quad (4)$$

The higher the $pL_{0.5}$, the higher the sequestering ability. Further details about the theoretical basis of this approach, on its determination and on its comparison with other methods can be found in ref. [2]. What is important to mention here is that: i) the fraction of complexed metal by a given ligand (and, therefore, the $pL_{0.5}$) can be easily determined by means of programs commonly used to build speciation plots (building the so-called sequestration diagrams); ii) in the way it is calculated, $pL_{0.5}$ takes into account the whole composition of the system, so that its value is dependent on the conditions of the system itself (*e.g.,* ionic strength, temperature, pH), but it is "cleaned" from all competing reactions occurring in the system itself, facilitating comparisons. For example, the sequestration diagrams and the $pL_{0.5}$ of the three NTAXP ligands toward the metal and organometal cations investigated in this work have been calculated at pH = 8.1 (always at $I = 0.1$ mol L^{-1} in $NaCl_{(aq)}$ and at $T = 298.15$ K): $pL_{0.5}$ are reported in Table 10, while Figure 9 shows, as an example, the sequestration diagrams of the three NTAXP ligands towards Hg^{2+} and CH_3Hg^+. In the above cited conditions, the greatest sequestering ability at all is shown by NTA2P towards Sn^{2+}, and NTA3P towards $(CH_3)_2Sn^{2+}$. Concerning NTAP, the greatest sequestering power is observed towards Hg^{2+}. Comparing the behaviour of the three separate NTAXP ligands towards the four cations, their sequestering ability is:

$Hg^{2+} > Sn^{2+} > (CH_3)_2Sn^{2+} > CH_3Hg^+$ for NTAP
$Sn^{2+} > Hg^{2+} > (CH_3)_2Sn^{2+} > CH_3Hg^+$ for NTA2P
$(CH_3)_2Sn^{2+} > Hg^{2+} > Sn^{2+} > CH_3Hg^+$ for NTA3P

This suggest the possibility of using one ligand or another for the selective sequestration of one or more of these cations, also in systems containing mixtures of them.
All the speculations done also confirm that the efficacy of the sequestration process is not evaluable exclusively by the stability of complexes or by the number of potential binding sites of the ligand, but it derives from a combination of factors. For example, pH control is important during the sequestration process: lowering pH reduces completion of hydrolysis reactions of the cations, but protonates the ligands (which are less available for complexation); increasing pH favour metal hydrolysis and the ligand deprotonation... the two processes (hydrolysis and protonation) have opposite effects.

Empirical relationships

Together with results already shown, another of the aims of this work, stated in the introduction, was that of "…investigating the effect of the replacement of the carboxylic group(s) of one of the simplest complexones (nitrilotriacetic acid, NTA) by phosphonic function(s)…".

Table 10. Sequestering ability of NTAXP ligands towards Hg^{2+}, CH_3Hg^+, Sn^{2+} and $(CH_3)_2Sn^{2+}$, at pH = 8.1, $I = 0.1$ mol L^{-1} and $T = 298.15$ K

L	Hg^{2+}	CH_3Hg^+	Sn^{2+}	$(CH_3)_2Sn^{2+}$
	$pL_{0.5}$			
NTAP	5.61	3.08	4.90	3.47
NTA2P	6.01	2.90	8.35	5.38
NTA3P	5.52	3.14	4.83	8.37

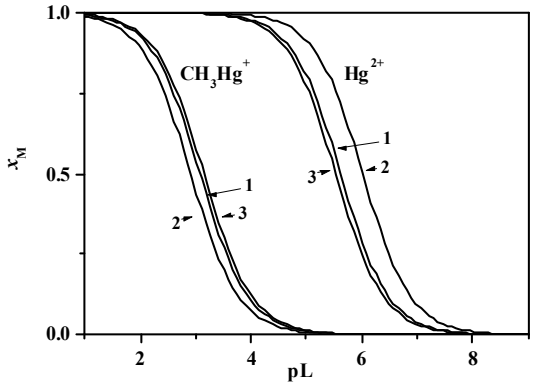

Figure 9. Sequestration diagrams of Hg^{2+} and CH_3Hg^+ by NTAP (1), NTA2P(2) and NTA3P(3) at pH = 8.1, in $NaCl_{(aq)}$ at $I = 0.1$ mol L^{-1} and $T = 298.15$ K.

From the comparison of the protonation constants of the three ligands (at I = 0.1 mo L^{-1}), together with those of NTA [25] in the same conditions, an interesting aspect emerges: the protonation constant of a given step is a regular function of the number of phosphonates (and, inversely, of the carboxylates) of the ligand (n_P), according to the following relationships (Figure 10):

$\log \beta_{011} = 9.31 + 1.37\ n_P - 0.17\ n_P^2$ $\quad r^2 = 0.998$
$\log \beta_{012} = 11.9 + 4.7\ n_P - 0.8\ n_P^2$ $\quad r^2 = 0.993$
$\log \beta_{013} = 13.4 + 6.0\ n_P - 0.8\ n_P^2$ $\quad r^2 = 0.995$
$\log \beta_{014} = 14.8 + 5.62\ n_P - 0.31\ n_P^2$ $\quad r^2 = 0.998$

Analogously, also the stability of the common metal complexes formed by both NTA and all the three NTAXP ligands with the cations investigated in the present work are regular function of n_P:

$$\log \beta_{pqr} = a + b\ n_P + c\ n_P^2 \quad (5)$$

Refined parameters of eq. (5), together with the corresponding correlation coefficients (r^2), are reported in Table 11, relatively only to the $M_pL_qH_r$ species common to all the four ligands (obviously relationships with three terms only are possible, but not significant and, therefore, have not been reported). As observed, this simple polynomial relationship, is valid for all the above-cited common species, and let one suppose that they could be equally exploited for an estimation of the stability constants of some species of these systems, which, for any reasons (like, *e.g.*, experimental limitations), have not been determined. For example, it has been discussed above that, due to solubility problems, measurements on the Sn^{2+} / NTA system have been performed considering ligand excesses that, in those conditions, favoured the formation of the dimeric species reported and hampered the determination of the stability constants of simple species. Nevertheless, these simple $Sn_p(NTA)_qH_r$ species could be formed in other conditions like, *e.g.*, in very diluted systems or in cases where $c_M > c_L$. In those situations, the availability of an estimated stability constant value of a given complex, though affected by high uncertainty, is always desirable instead of having no idea about it. By this approach, considering the ML species of the three NTAXP ligands (NTA is missing), it is expected that the stability constant of the simple $Sn(NTA)^-$ species would be log $\beta_{110} \sim 12.0$.

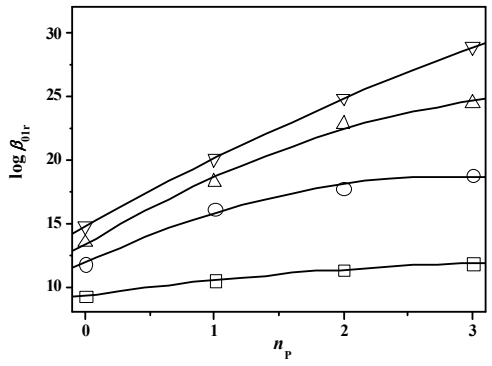

Figure 10. Protonation constants (log β_{01r}) of NTAXP ligands, as a function of the number of phosphonates (n_P), in $NaCl_{(aq)}$ at I = 0.1 mol L^{-1}, and at T = 298.15 K. Squares: r = 1; Circles: r = 2; Up triangles: r = 3; Down triangles: r = 4.

Conclusions

In this paper, the results on an investigation on the complexation of Hg^{2+}, CH_3Hg^+, Sn^{2+}, and $(CH_3)_2Sn^{2+}$ by NTAP, NTA2P, and NTA3P, have been reported, as a further contribution of this group to the knowledge and modelling of the speciation of these four cations in real systems of biological, environmental, and technological/industrial interest containing different ligands. Some examples are represented by refs. [41-47] for Hg^{2+} and CH_3Hg^+, while refs. [7, 18, 48-51] may be considered for Sn^{2+}, and $(CH_3)_2Sn^{2+}$. Moreover, the systematic changes in the ligand structure of investigated ligands allowed the modelling of the effect of the number of carboxylic and/or phosphonic groups of the ligand(s) on its (their) binding ability, by means of simple polynomial functions. In addition, their sequestering ability has been quantified by means of the calculation of the parameter $pL_{0.5}$, since this aspect cannot be easily assessed by the simple comparison of the stability constants of various complexes. From $pL_{0.5}$ analysis, it emerged that the three NTAXP ligand behave differently towards Hg^{2+}, CH_3Hg^+, Sn^{2+}, and $(CH_3)_2Sn^{2+}$. For example, at pH 8.1, the "best" sequestering agent for Hg^{2+} and Sn^{2+} is NTA2P, while NTA3P is the best for CH_3Hg^+ and $(CH_3)_2Sn^{2+}$.
Finally, from measurements at variable ionic strengths and temperatures, it emerged that the latter has little effect on the speciation of the ligands, while the formed deeply affect that of the cations investigated.

Acknowledgements

The authors thank the university of Messina for partial financial support.

Table 11. Empirical parameters of eq. (5) for the modelling of the dependence of the stability constants of various $M_p(NTAXP)_qH_r$ species on the number of phosphonic groups (n_P) of the ligand, in $NaCl_{(aq)}$ at I = 0.1 mol L^{-1}, and at t = 25 °C

M	Species [a]	a	b	c	r^2
Hg^{2+}	1 1 0	14.46	6.42	-1.40	0.984
CH_3Hg^+	1 1 1	15.94	1.09	-0.06	0.993
CH_3Hg^+	1 1 0	9.05	0.97	-0.11	0.996
$(CH_3)_2Sn^{2+}$	1 1 1	12.42	4.48	-0.08	0.999
$(CH_3)_2Sn^{2+}$	1 1 0	10.22	3.39	-0.11	0.999
$(CH_3)_2Sn^{2+}$	1 1 -1	3.21	-1.57	1.44	0.999

[a] index refer to equilibria: p M + q NTAP + r H = $M_p(NTAP)_qH_r$

References

1. G. Drasch, M. Horvat and M. Stoeppler, in *Elements and Their Compounds in the Environment*, Wiley-VCH Verlag GmbH, 2004, DOI: 10.1002/9783527619634.ch38, pp. 931-1005.
2. F. Crea, C. De Stefano, C. Foti, D. Milea and S. Sammartano, *Curr. Med. Chem.*, 2014, **21**, 3819-3836.
3. Mercury. U.S. Environmental Protection Agency, http://www.epa.gov/earlink1/mercury/index.html, (accessed July 2015, 2015).
4. Mercury. World Health Organization - International Programme on Chemical Safety, http://www.who.int/ipcs/assessment/public_health/mercury/en/, (accessed July 2015, 2015).
5. Mercury. UNEP - United Nations Environment Programme, http://www.unep.org/hazardoussubstances/Mercury/tabid/434/Default.aspx, (accessed July 2015, 2015).
6. F. Cima, P. J. Craig and C. F. Harrington, in *Organometallic Compounds in the Environment*, John Wiley & Sons, Ltd, 2003, DOI: 10.1002/0470867868.ch3, pp. 101-149.
7. A. Gianguzza, O. Giuffrè, D. Piazzese and S. Sammartano, *Coord. Chem. Rev.*, 2012, **256**, 222-239.
8. J. P. Anger, in *Elements and their Compounds in the Environment. 2nd. Edition.*, eds. E. Merian, M. Anke, M. Ihnat and M. Stoeppler, Wiley-VCH Verlag GmbH & Co. KGaA, Weinheim, 2004, pp. 1113-1124.
9. K. Popov, H. Ronkkomaki and L. H. J. Lajunen, *Pure Appl. Chem.*, 2001, **73**, 1641-1677.
10. K. S. Popov, H. Ronkkomaki and L. H. J. Lajunen, *Pure Appl. Chem.*, 2002, **74**, 2227.
11. B. Nowack, *Water Res.*, 2003, **37**, 2533-2546.
12. J. Galezowska and E. Gumienna-Kontecka, *Coord. Chem. Rev.*, 2012, **256**, 105-124.
13. C. Foti, O. Giuffrè and S. Sammartano, *J. Chem. Thermodynamics*, 2013, **66**, 151-160.
14. R. M. Cigala, M. Cordaro, F. Crea, C. De Stefano, V. Fracassetti, M. Marchesi, D. Milea and S. Sammartano, *Ind. Eng. Chem. Res.*, 2014, **53**, 9544-9553.
15. C. De Stefano, G. Lando, A. Pettignano and S. Sammartano, *J. Mol. Liquid*, 2014, **199**, 432-439.
16. C. De Stefano, G. Lando, A. Pettignano and S. Sammartano, *J. Chem. Eng. Data*, 2014, **59**, 1970–1983.
17. R. M. Cigala, F. Crea, C. De Stefano, G. Lando, D. Milea and S. Sammartano, *Geochim. Cosmochim. Acta*, 2012, **87**, 1-20.
18. D. Cucinotta, C. De Stefano, O. Giuffrè, G. Lando, D. Milea and S. Sammartano, *J. Mol. Liq.*, 2014, **200**, 329-339.
19. C. De Stefano, C. Foti, O. Giuffrè and S. Sammartano, *J. Chem. Eng. Data*, 2001, **46**, 1417-1424.
20. C. De Stefano, S. Sammartano, P. Mineo and C. Rigano, in *Marine Chemistry - An Environmental Analytical Chemistry Approach*, eds. A. Gianguzza, E. Pelizzetti and S. Sammartano, Kluwer Academic Publishers, Amsterdam, 1997, pp. 71-83.
21. P. Gans, Hyperquad, http://www.hyperquad.co.uk/, (accessed Accessed May 2015, 2015).
22. K. J. Powell, P. L. Brown, R. H. Byrne, T. Gajda, G. Hefter, S. Sjöberg and H. Wanner, *Pure Appl. Chem.*, 2005, **77**, 739-800.
23. A. De Robertis, C. Foti, G. Patanè and S. Sammartano, *J. Chem. Eng. Data*, 1998, **43**, 957-960.
24. C. De Stefano, C. Foti, A. Gianguzza, M. Martino, L. Pellerito and S. Sammartano, *J. Chem. Eng. Data*, 1996, **41**, 511-515.
25. P. G. Daniele, C. Rigano and S. Sammartano, *Analytical Chem.*, 1985, **57**, 2956-2960.
26. A. E. Martell, R. M. Smith and R. J. Motekaitis, *NIST Standard Reference Database 46, vers.8*, Gaithersburg, 2004.
27. K. Sawada, W. Duan, M. Ono and K. Satoh, *J. Chem. Soc., Dalton Trans.*, 2000, DOI: 10.1039/A909207B, 919-924.
28. S. Cataldo, C. De Stefano, A. Gianguzza and A. Pettignano, *J. Mol. Liquid*, 2012, **172**, 46-52.
29. L. G. Sillén and A. E. Martell, *Stability Constants of Metal Ion Complexes. Special Publ. 17.*, The Chemical Society, Wiley, London, 1964.
30. L. G. Sillén and A. E. Martell, *Stability Constants of Metal Ion Complexes. Supplement Special Publ. 25.*, The Chemical Society, Wiley, London, 1964.
31. E. Hogfeldt, *Stability Constants of Metal-ion Complexes. Par. A: Inorganic Ligands. IUPAC Chemical Data Series*, Pergamon Press, Oxford, 1982.
32. D. Pettit and K. Powell, *IUPAC Stability Constants Database*, Academic Software, Otley, UK, 2004.
33. P. M. May, D. Rowland, E. Königsberger and G. Hefter, *Talanta*, 2010, **81**, 142-148.
34. S. Cataldo, C. De Stefano, A. Gianguzza, A. Pettignano and S. Sammartano, *J. Mol. Liquid*, 2013, **187**, 74–82.
35. C. Lentner, *Geigy Scientific Tables, 8th ed.*, CIBA-Geigy, Basilea, Switzerland, 1983.
36. J. Buffle, *Complexation Reactions in Aquatic Systems: an Analytical Approach*, Ellis Horwood, Chichester, 1988.
37. F. M. M. Morel and J. G. Hering, *Principles and Applications of Aquatic Chemistry (2nd ed.)*, John Wiley & Sons, Inc., New York, 1993.
38. W. Stumm and J. J. Morgan, *Aquatic Chemistry. Chemical Equilibria and Rates in Natural Waters. 3rd ed.*, John Wiley & Sons, Inc., New York, 1996.
39. I. Grenthe and I. Puigdomenech, *Modelling in Aquatic Chemistry*, OECD, Paris, 1997.
40. F. J. Millero, *Physical Chemistry of Natural Waters*, John Wiley & Sons, Inc., New York, 2001.
41. C. De Stefano, D. Milea, N. Porcino and S. Sammartano, *J. Agric. Food Chem.*, 2006, **54**, 1459-1466.
42. C. Foti, O. Giuffrè, G. Lando and S. Sammartano, *J. Chem. Eng. Data*, 2009, **54**, 893–903.
43. P. Cardiano, D. Cucinotta, C. Foti, O. Giuffrè and S. Sammartano, *J. Chem. Eng. Data*, 2011, **56**, 1995-2004.
44. P. Cardiano, G. Falcone, C. Foti, O. Giuffrè and S. Sammartano, *New J. Chem.*, 2011, **35**, 800 - 806.
45. P. Cardiano, G. Falcone, C. Foti and S. Sammartano, *J. Chem. Eng. Data*, 2011, **56**, 4741-4750.
46. G. Falcone, C. Foti and S. Sammartano, *J. Chem. Eng. Data*, 2012, **57**, 3636−3643.
47. G. Falcone, C. Foti, A. Gianguzza, O. Giuffrè, A. Napoli, A. Pettignano and D. Piazzese, *Anal. Bioanal. Chem.*, 2013, **405**, 881-893.
48. C. De Stefano, D. Milea and S. Sammartano, *Biophys. Chem.*, 2005, **116**, 111-120.
49. R. M. Cigala, F. Crea, C. De Stefano, G. Lando, D. Milea and S. Sammartano, *J. Chem. Thermodyn.*, 2012, **51**, 88–96.
50. P. Cardiano, G. Falcone, C. Foti, O. Giuffrè and A. Napoli, *J. Inorg. Biochem.*, 2013, **129**, 84-93.
51. R. M. Cigala, F. Crea, C. De Stefano, D. Milea, S. Sammartano and M. Scopelliti, *Monatsh. Chem.*, 2013, **144**, 761-772.

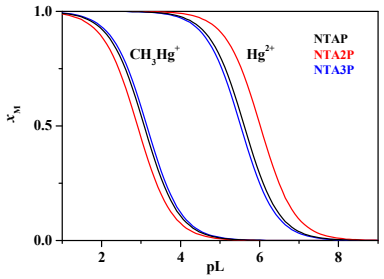

Replacing carboxylic by phosphonic groups in NTA significantly affects the sequestering ability toward Hg^{2+}, CH_3Hg^+, Sn^{2+}, and $(CH_3)_2Sn^{2+}$